Stacking-Unstacking of the Dinucleoside Monophosphate Guanylyl-3′,5′-Uridine Studied with Molecular Dynamics

Jan Norberg* and Lennart Nilsson
Karolinska Institute, Center for Structural Biochemistry, Novum Research Park, S-141 57 Huddinge, Sweden

ABSTRACT Molecular dynamics simulations were carried out on two conformations of the dinucleoside monophosphate guanylyl-3′,5′-uridine (GpU) in aqueous solution with one sodium counterion. One stacked conformation and one with the C3′-O3′-P-O5′ backbone torsion angle twisted 180° to create an unstacked conformation. We observed a relatively stable behavior of the stacked conformation, which remained stacked throughout the simulation, whereas the unstacked conformation showed major changes in the backbone torsion and glycosidic angles. During the simulation the unstacked conformation transformed into a more stacked form and then back again to an unstacked one. The calculated correlation times for rotational diffusion from the molecular dynamics simulations are in agreement with fluorescence anisotropy and nuclear magnetic resonance data. As expected, the correlation times for rotational diffusion of the unstacked conformation were observed to be longer than for the stacked conformation. The 2′OH group may contribute in stabilizing the stacked conformation, where the O2′-H···O4′ hydrogen bond occurred in 82.7% of the simulation.

INTRODUCTION

Structural features and internal dynamics of nucleic acids are important for understanding their physical properties and biological functions. One very characteristic feature of nucleic acids is the ability of the bases to stack on top of each other, a phenomenon which has been extensively studied using dinucleoside monophosphates as model systems. The conformation of dinucleoside monophosphates is determined by factors such as ionization state, solvation, counterions and temperature. The base-base stacking resulting from π-π interactions between aromatic molecules is mainly stabilized by London dispersion forces and hydrophobic effects (Saenger, 1988). The π-π interactions have been divided into four contributions to take into account the electrostatic interactions with the π-electron density above and below the planes of the aromatic bases: the van der Waals interactions, the electrostatic interactions between partial atomic charges, the electrostatic interactions between the charge distributions associated with the out-of-plane π-electron density, and the electrostatic interactions between the charge distributions associated with the out-of-plane π-electron density and the partial atomic charges (Hunter, 1993). Conformational changes and thermodynamics of dinucleoside monophosphates have been studied by a variety of experimental and theoretical methods, circular dichroism (CD), optical rotatory dispersion (ORD), nuclear magnetic resonance (NMR), and molecular dynamics (MD). Early optical studies (Warshaw and Tinoco, 1966) have suggested that adenine, cytosine and guanine stack but not uracil and that if both bases of the dinucleoside monophosphate were equally charged they would become unstacked. This is consistent with a self-association study (Ts'o et al., 1963), where uracil has the least tendency to stack and the stacking ability of dinucleoside monophosphates decreases in the following order: purine-purine > purine-pyrimidine > pyrimidine-pyrimidine. Eight types of stacking interactions of the nucleic acid bases are proposed by stoichiometric considerations (Lysov et al., 1979). CD experiments of GpU and 17 GpU analogues (Guschlbauer et al., 1972) have shown that GpU is very little stacked at room temperature and neutral pH, but at low temperature and low pH stacking occurs. It has been shown that stacking occurs upon protonation of the nitrogen at position 7 of the guanine base (N7) at pH 1, G^+pU (Warshaw and Tinoco, 1966). In contrast the dinucleoside monophosphate UpG stacks at pH 7 as well as at pH 1 upon protonation, UpG^+. GpU has been extensively investigated by nuclear magnetic resonance experiments (Chachaty et al., 1977; Ts'o et al., 1969). From proton magnetic resonance data it has first been concluded that all dinucleoside monophosphates are in a right-handed anti-anti-conformation (Ts'o et al., 1969) but later some exceptions have been shown to exist, for instance GpU and GpC (Chachaty et al., 1977; Neumann et al., 1979), where it has been quite clearly shown that the orientation is predominantly syn for the Guo moiety and anti for the Urd moiety (Chachaty et al., 1977). At room temperature and neutral pH an unusual perpendicular structure of GpU has been proposed (Guschlbauer et al., 1971; Guschlbauer et al., 1972) with Guo in syn and Urd in anti. This structure may also involve a hydrogen bond between the 2-amino group of Guo and the 4-keto group of Urd. The syn conformation of Guo could also be stabilized by the free O5′H hydroxyl which can form a hydrogen bond O5′H···N3 (Saenger, 1988).

Received for publication 11 February 1994 and in final form 11 May 1994.

Address reprint requests to Dr. Jan Norberg, Karolinska Institute, Center for Structural Biochemistry, Novum Research Park, S-141 57 Huddinge, Sweden. Tel: 46-8-608-9264; Fax: 46-8-608-9290; E-mail: jan.norberg@csb.ki.se.

Abbreviations used: GpU, guanylyl-3′,5′-uridine; Gua, guanine; Ura, uracil; Guo, guanosine; Urd, uridine; 2aPU, 2-amino-purine uracil; MD, molecular dynamics; NMR, nuclear magnetic resonance; CD, circular dichroism; RMS, root-mean-square.

0006-3495/94/08/812/13 $2.00

The overall motion of dinucleoside monophosphates are in the picosecond to nanosecond range and can be studied both with NMR and fluorescence anisotropy measurements. In NMR experiments, the relaxation of all protons of the molecule are governed by the same correlation time and in a NMR study of GpU the correlation times of Gp and pU have been determined (Chachaty et al., 1977). The correlation times have also been determined for the 5′-nucleotides 5′GMP and 5′UMP (Chachaty et al., 1976). The correlation times for the rotational diffusion can also be determined from fluorescence anisotropy measurements knowing the transition moment of the molecule. In some previous studies molecular dynamics simulations have been used to verify fluorescence anisotropy measurements (Ichiye and Karplus, 1983; Hu and Fleming, 1991).

Theoretical studies of stacking interactions between nucleic acid bases have been made using a multipole approach (Langlet et al., 1981) and potential energy calculations of deoxydinucleoside phosphate complexes have been carried out to examine the low-energy conformations (Poltev et al., 1981). One theoretical tool that has been used to gain insight into the dynamic behavior of molecules and to describe and predict the structure of biological molecules is molecular dynamics simulation (Brooks et al., 1988; McCammon and Harvey, 1987). Relatively long simulations under realistic solvent conditions have been used to characterize the conformational dynamics of oligopeptides and protein fragments (Tobias et al., 1991; Soman et al., 1991; DiCapua et al., 1991; De Loof et al., 1992). Since the start in 1983 of molecular dynamics (MD) simulations of nucleic acids in vacuo (Levitt, 1983; Prabhakaran et al., 1983; Tidor et al., 1983) and with inclusion of explicit solvent (Seibel et al., 1986; van Gunsteren et al., 1986) investigations of nucleic acids using MD simulations have increased enormously. In this work, molecular dynamics simulations have been performed on two different starting conformations of the dinucleoside monophosphate GpU in aqueous solution. One simulation was carried out for a stacked conformation and the other for an extended or unstacked conformation. The results from the simulations are compared to fluorescence anisotropy measurements for a very similar fluorescent compound, the dinucleoside monophosphate 2-aminopurine uracil (2aPU) (R. Rigler and T. Kulinski, personal communication) and to nuclear magnetic resonance data on GpU (Chachaty et al., 1977). The conformational changes of the backbone torsion angles, the glycosidic angles, and the sugar moieties have been investigated. Focusing on the correlation times for rotational diffusion for the two conformations it would be possible to predict the equilibrium relationship of the stacking-unstacking process. This study is part of a set of investigations of the dinucleoside monophosphate GpU, concerned with the effects of various simulation parameters including water models, force fields, boundary conditions, and different temperatures.

MATERIALS AND METHODS

Simulation protocol

The CHARMM program (Brooks et al., 1983) with the standard nucleic acid parameters (Nilsson and Karplus, 1986) was used for the energy minimizations and MD simulations. The starting structure for the dinucleoside monophosphate guanylyl-3′,5′-uridine (GpU) was made from x-ray fiber diffraction analysis (Arnott et al., 1976). Hydroxy groups have been added at the 5′ and the 3′ terminals. The united atom model was used for all hydrogens attached to carbon atoms and all other hydrogens were treated explicitly. Two different conformations of the GpU were used in the investigation, one stacked conformation and one conformation with the ζ torsion angle (Saenger, 1988) twisted 180° to have it in an extended or unstacked form (Fig. 1). The stacked conformation was also studied in a deoxy form, where the hydroxy groups at the C2′ position of the sugar were changed to hydrogens. Each system was made electrically neutral by adding a sodium counterion. Initially the counterion was placed along the O-P-O bisector, 1.48 Å from each oxygen atom and 1.57 Å from the phosphorus atom. The systems were first energy minimized with 100 cycles of steepest descent (SD) and thereafter 3000 cycles of adopted-basis set Newton-Raphson (ABNR) (Brooks et al., 1983). The sodium counterion moved during the minimizations symmetrically away from the oxygen atoms to a distance of 2.23 Å for the stacked conformation and 2.26 Å for the extended.

The solute (GpU) with the counterion was placed in the center of mass of a box of water generated from the TIP3P water model (Jorgensen et al., 1983). All water molecules which had the oxygen atom closer than 2.8 Å to any heavy atom of the solute molecules were deleted to avoid overlap between solute and water molecules. Periodic boundary conditions were applied using a cubic box with side length 25.0 Å for the stacked conformation of GpU and d(GpU), and a rectangular box with side lengths 28.0, 31.1, and 31.1 Å for the unstacked GpU conformation. The water molecules of the boxes were energy minimized with 100 cycles of SD and 3000 cycles of ABNR, while constraining the solute and the counterion to their original positions by a harmonic potential with a force constant of 1.0 kcal·mol^{-1}·Å^{-2}. The SHAKE algorithm (Ryckaert et al., 1977; van Gunsteren and Berendsen, 1977) was used to constrain all the bonds and to allow for a time step of 2 fs during the integration, for which we used the Verlet algorithm (Verlet, 1967). The coordinates were saved every 50 steps. The dielectric constant was set to 1.0 and the non-bonded interactions were shifted to smoothly approach 0 at 8.5 Å (Brooks et al., 1983). The non-bonded atom-based list was updated every 10 steps with a cut-off of 9.0 Å. The temperature of the systems was increased from 100 K to 300 K in increments of 10 K during the first 2 ps. The MD simulation of the stacked conformation was continued for 998 ps after the heating period giving a total simulation length of 1.0 ns and the MD simulation of the unstacked conformation was continued for 1998 ps and for a total of 2.0 ns. The MD simulation of the deoxy form was carried out for 200 ps and has only been analyzed regarding the stacking and the hydrogen bonding. These MD simulations are carried out for a relatively long time to ensure that the whole conformational space has been covered. All the MD simulations were performed on IBM RISC 6000 workstations.

Radius of gyration

The deformations of the dinucleoside monophosphate during the MD simulations can be monitored by calculation of the radius of gyration. The radius of gyration is defined through

$$r_G^2 = \frac{\sum_{i=1}^{n} m_i r_i^2}{\sum_{i=1}^{n} m_i} \quad (1)$$

where m_i is the mass of the ith atom, r_i is the distance from the ith atom to the center of mass, and n is the number of atoms in the molecule. For a uniform sphere of radius r, the radius of gyration (Marshall, 1978) is $r_G = (\frac{3}{5})^{1/2} \cdot r$.

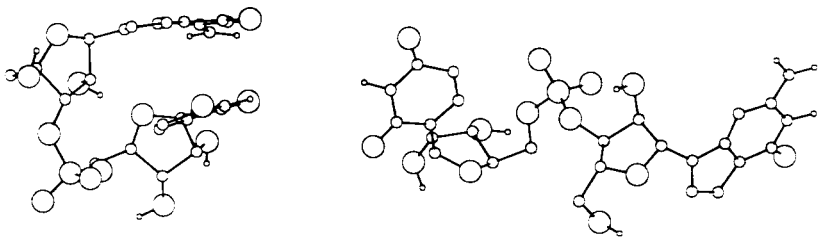

FIGURE 1 An illustration of the conformations used as starting structures of the MD simulations. The stacked (*left*) and the unstacked (*right*) conformation.

Rotational diffusion

Information about rotational diffusion can be obtained from the fluorescence emission anisotropy decay, $r(t)$, which measures the autocorrelation of the second-order Legendre polynomial $P_2(x)$:

$$r(t) = \tfrac{2}{5}\langle P_2[\hat{\mu}_A(0) \cdot \hat{\mu}_E(t)]\rangle \tag{2}$$

where $\hat{\mu}_A(0)$ is the absorption dipole moment at time 0 and $\hat{\mu}_E(t)$ is the emission dipole moment at time t of the chromophore. The fluorescence depolarization of the molecule comes from the ensemble average of the correlation function (Ichiye and Karplus, 1983), which is estimated by

$$\langle P_2[\hat{\mu}_A(0) \cdot \hat{\mu}_E(t_m)]\rangle \approx \frac{1}{N-m}\sum_{n=1}^{N-m} P_2[\hat{\mu}_A(t_n) \cdot \hat{\mu}_E(t_n + t_m)] \tag{3}$$

where N and m are the total number of time steps and intermediate time steps in the molecular dynamics simulation. The naturally occurring nucleic acid bases are only weakly luminescent and under normal conditions it is usually necessary to use some fluorescent probe. The dinucleoside monophosphate 2-amino purine uracil (2aPU) has been studied using fluorescence anisotropy measurements by R. Rigler and T. Kulinski (personal communication). This compound contains the fluorescent 2-amino purine and is very similar to the guanylyl-3′,5′-uridine monophosphate (GpU) used in our simulations. The overall similarity between these two molecules makes it possible to compare correlation times for the rotational diffusion from molecular dynamics simulations with fluorescence anisotropy measurements. The correlation times for the rotational diffusion have been calculated to characterize the overall motion of the dinucleoside monophosphate GpU. To evaluate the fluorescence anisotropy from the molecular dynamics trajectory, one needs to know the orientations of the transition moments $\hat{\mu}_A$ and $\hat{\mu}_E$ for 2-amino purine. Preliminary data indicate that 2-amino purine has two transition moments at ±40° to a vector between the C8 atom and the average position of the N1 and C2 atoms (B. Albinsson and B. Nordén, personal communication).

To estimate the overall motion of the dinucleoside monophosphate the correlation time for rotational diffusion can be determined. We have calculated the reorientation correlation functions for vectors connecting two atoms according to

$$C_j(t) = \langle P_j(\cos\theta(\tau, t))\rangle_\tau \tag{4}$$

where $\theta(\tau, t)$ is the angle between the vector at a time τ and the same vector at a time t later and P_j is the Legendre polynomial of order j. When $C_j(t)$ decays as a single exponential the rotational correlation time τ_c can be calculated using $C_j(t) = A\exp(-t/\tau_c)$, where A is a constant and t is the time.

The rotational diffusion correlation times were also estimated using the hydrodynamic model. The rotational diffusion coefficient D_{rot} is related to the rotational frictional coefficient f_{rot} by the Stokes-Einstein formula (Marshall, 1978), $D_{rot} = kT/f_{rot}$, where k is the Boltzmann constant and T is the temperature. For a sphere of radius r the relation between the rotational friction coefficient, the molecular size and the solution viscosity is $f_{rot} = 8\pi\eta_0 r^3$. In the case of fluorescence depolarization the correlation time of rotational diffusion τ_c is related to the rotational diffusion constant by $\tau_c = (6D_{rot})^{-1}$. The correlation time of rotational diffusion τ_c of a sphere can then be calculated using $\tau_c = (4\pi\eta_0 r^3/3kT)$, where η_0 is the viscosity of water at 300 K and r is the Stokes effective radius. In hydrodynamic measurements of non-spherical molecules it is not possible to use a single rotational frictional coefficient; instead, two coefficients are used for ellipsoids (Cantor and Schimmel, 1980). The rotational frictional coefficients f_a and f_b around the long and the short semiaxes a and b, respectively, are defined relative to the rotational frictional coefficient f_{rot} of a sphere of equivalent volume

$$f_a = \frac{4(1-p^2)}{3(2-p^2S)} f_{rot} \quad \text{and} \quad f_b = \frac{4(1-p^4)}{3p^2[S(2-p^2)-2]} f_{rot} \tag{5}$$

where S and p are defined as follows:

$$S = \frac{2}{\sqrt{1-p^2}} \ln\left[\frac{1+\sqrt{1-p^2}}{p}\right] \quad \text{and} \quad p = \frac{b}{a} \tag{6}$$

for a prolate ellipsoid. The rotation of prolate ellipsoids about their short axes b involve great friction. The correlation times for rotation about the long axis and the short axis are defined as

$$\tau_a = \frac{f_b}{f_{rot}}\tau_c \quad \text{and} \quad \tau_b = \frac{2}{f_{rot}}\left[\left(\frac{1}{f_a}\right) + \left(\frac{1}{f_b}\right)\right]^{-1}\tau_c \tag{7}$$

where τ_c is the correlation time for rotation of a sphere of equivalent volume.

RESULTS AND DISCUSSION

Backbone torsion and glycosidic angles

The C3′-O3′-P-O5′ backbone torsion angle ζ of the stacked conformation of the dinucleoside monophosphate GpU was twisted 180° to create the unstacked conformation (Fig. 1). The average of the backbone torsion angles over the last 400 ps are reported in Table 1 for both MD simulations (except for the glycosidic angle of the Guo moiety, see Fig. 2, where the last 350 ps were used due to a major transition).

Naturally both the backbone torsion angles and the glycosidic angles of the stacked conformation showed average values close to those of the x-ray fiber diffraction structure of A-RNA (Arnott et al., 1972; Saenger, 1988). In the MD

TABLE 1 Backbone torsion and glycosidic angles

Angles*	Stacked conformation	Extended conformation	A-RNA*
γ (Gua)	59.6 (9.1)	62.0 (8.8)	54.0
δ (Gua)	73.7 (7.3)	68.8 (7.2)	82.0
ε	−162.5 (10.6)	−162.3 (9.2)	−153.0
ζ	−71.5 (9.7)	72.8 (12.1)	−71.0
α	−67.3 (11.1)	−175.3 (11.1)	−68.0
β	163.3 (11.0)	242.6 (18.6)	178.0
γ (Ura)	58.7 (7.6)	66.4 (7.8)	54.0
δ (Ura)	80.3 (6.9)	80.0 (6.6)	82.0
χ (Gua)	−153.3 (15.3)	−261.8 (15.2)	−158.0
χ (Ura)	−144.2 (14.3)	−121.6 (21.9)	−158.0

Values in the parentheses are the standard deviation.
* From Saenger (1988).

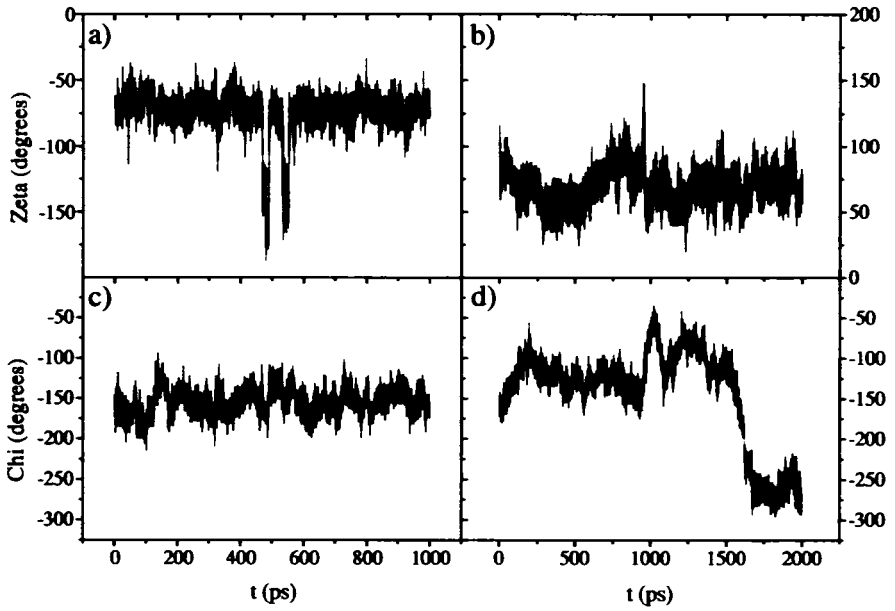

FIGURE 2 The trajectory of the ζ (O5′-P-O3′-C3′) torsional angle for the stacked (*a*) and the unstacked (*b*) conformation and the trajectory of the χ (O4′-C1′-N9-C4) torsional angle of the guanosine moiety for the stacked (*c*) and the unstacked (*d*) conformation.

simulation of the stacked conformation two transitions occurred, one just before 500 ps and the other just after 500 ps (Fig. 2 *a*).

These transitions could be followed through some of the backbone torsion angles: α, β, ϵ, and ζ. The δ and γ backbone torsion angles showed no transitions and had the smallest root-mean-square (RMS) fluctuations during the MD simulation. The dynamical behavior of the backbone torsion and the glycosidic angles has been plotted in Fig. 3 using the program Dials and Windows (Ravishanker et al., 1989). The time evolution, with $t = 0$ ps at the center of the circle, of the angles are displayed using dials with 0° at the top and the angles increase in the clockwise direction.

If we look at the MD simulation of the unstacked conformation the same behavior was observed concerning the δ and γ backbone torsion angles as for the MD simulation of the stacked conformation. The ϵ torsion angle of the unstacked conformation showed no major changes, but the α torsion angle made one major change from an average of $-63.3°$ during the first 750 ps to an average of $-173.7°$ during the last 1100 ps. The 180° disturbed ζ torsion angle showed one transition, which occurred during the period 945–960 ps (Fig. 2 *b*). The β torsion angle made a couple of large transitions, one at 150 ps and another transition at 750 ps, to an average of 242.6° the last 400 ps. The glycosidic angle χ defines the orientation of the base relative to the sugar (Saenger, 1988). The χ_{Gua} and the χ_{Ura} angles of the stacked and the unstacked conformation showed large RMS fluctuations, about 15° in the stacked case and 14–22° in the unstacked case (Table 1). The χ_{Gua} angle of the stacked conformation did not show any major transition (Fig. 2 *c*) as was observed for the unstacked conformation at 1600 ps (Fig. 2 *d*). NMR relaxation and CD results have shown that Guo has a preference for the syn conformation, while the Urd

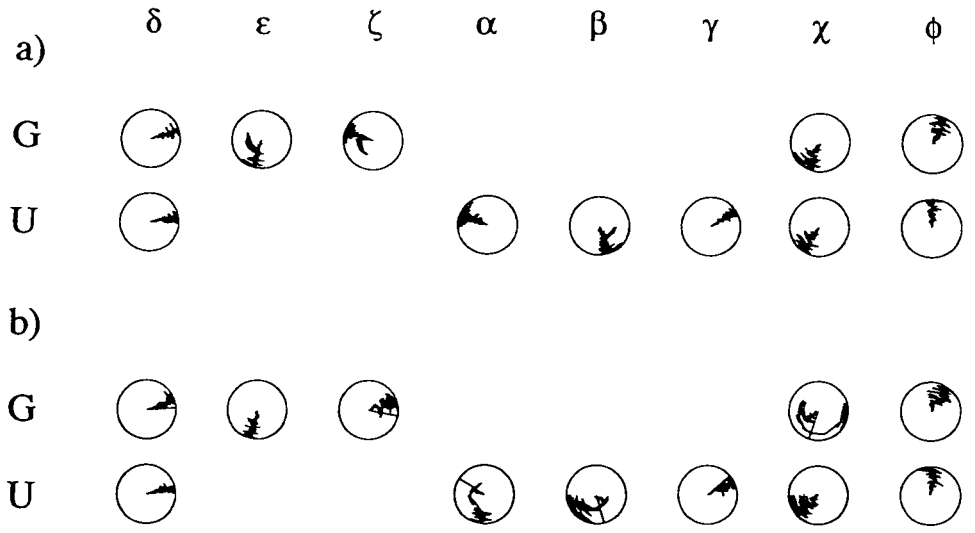

FIGURE 3 Time evolution of the backbone torsional angles, the glycosidic torsional angles (χ), and the sugar pucker pseudorotation phase angles (ϕ) of the guanylyl-3′,5′-uridine for the stacked (*a*) and the unstacked (*b*) conformation.

moiety is in the anti orientation (Chachaty et al., 1977; Guschlbauer et al., 1972). Potential energy calculations (Yathindra and Sundaralingam, 1973) also led to the conclusion that Guo is in the syn conformation. The anti form of both the Guo and the Urd moiety was observed in the MD simulation of the stacked conformation, whereas for the unstacked conformation the Guo and Urd moieties were in the syn conformation 18.2% and 10.3% of the MD simulation, respectively.

Radius of gyration

In the case of the stacked conformation the radius of gyration (Eq. 1) showed no large changes during the 1.0 ns MD simulation (Fig. 4 *a*) with an average of 4.02 Å and a RMS fluctuation of 0.08 Å during the last 400 ps. The radius of gyration of the unstacked conformation fluctuated over an interval of ~1.6 Å during the whole 2.0-ns MD simulation (Fig. 4 *b*).

The unstacked GpU expanded approximately 0.4 Å in the first 200 ps, followed by a contraction period of 80 ps, where the radius of gyration decreased to 4.4 Å. During this period the GpU transformed into a more stacked form. An expansion period started at 580 ps and thereafter two contraction-expansion periods could be observed, one between 1060 ps and 1250 ps and the other from 1600 ps to 2000 ps. The last contraction period depended on a major transition of the glycosidic torsion angle of the guanosine base (Fig. 2 *d*) and the final expansion from 1890 ps was caused by the glycosidic torsion angle of the uridine moiety. The radius of gyration was also calculated using the formula of a uniform sphere, to see if a spherical approximation of the stacked conformation could be used. If half the longest intramolecular distance was used as the radius, we got a radius of gyration of 4.26 Å, which is about 0.2 Å (6%) larger than the value from Eq. 3.

Accessible surface area

The concept of solvent accessible surface area was first introduced to estimate the relative changes in the solvent accessible surface upon folding processes of polymers and also to determine the proportion of buried and exposed atomic groups (Lee and Richards, 1971). The solvent accessible surface area of nucleic acids was calculated using a spherical probe of radius r_w, 1.4 Å, corresponding to the average radius of a water molecule (Alden and Kim, 1979). The accessible surface area of the stacked starting conformation was 607.2 Å^2 and fluctuated around the average of 627.1 Å^2 during the last 400 ps (Fig. 4 *c*). On the other hand the unstacked conformation showed major changes of the accessible surface area and this has been plotted as a function of time in Fig. 4 *d*. The unstacked starting conformation has an accessible surface area of 735.3 Å^2. Three minima could be observed in the time dependence of the accessible surface area of the unstacked conformation, one in the region of 280–580 ps, another around 1180 ps, and the third during the period from 1600 ps to 2000 ps. The accessible surface area varied from 646.8 Å^2 to 770.2 Å^2 depending on the folding of the GpU. The accessible surface area was also calculated for different atom types, due to the fact that not all the atoms in the dinucleoside monophosphate simultaneously achieve their maximal exposure. The exposures of different atom types are listed in Table 2.

The accessible surface area of the different atom types of the stacked conformation showed small deviations from the starting conformation during the last 400 ps. The exposure

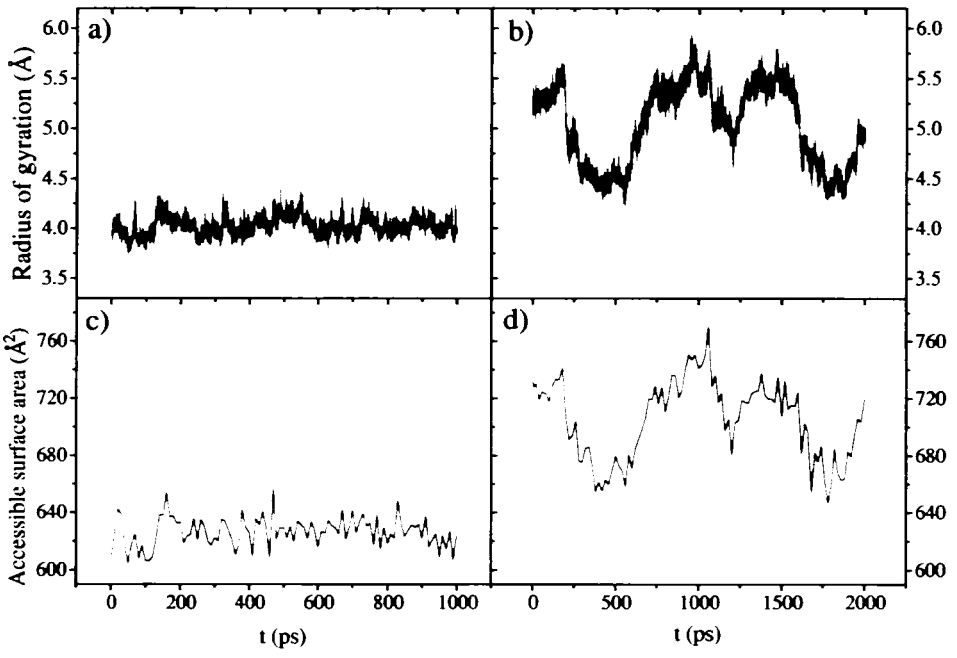

FIGURE 4 The radius of gyration vs. time for the stacked (*a*) and the unstacked (*b*) conformation. The accessible surface area vs. time for the stacked (*c*) and the unstacked (*d*) conformation.

TABLE 2 Accessible surface area of various atom types

Group type	Stacked starting conformation		Stacked conformation* 600–1000 ps		Unstacked starting conformation		Unstacked conformation* 380–480 ps		Unstacked conformation* 960–1060 ps	
	(Å²)	(%)	(Å²)	(%)	(Å²)	(%)	(Å²)	(%)	(Å²)	(%)
ALC	113.6	18.7	116.2	18.5	112.4	15.3	88.8	13.4	115.4	15.4
ARC	63.0	10.4	65.4	10.4	96.4	13.1	75.3	11.4	108.9	14.5
AMN	26.6	4.4	32.3	5.2	45.9	6.2	45.4	6.9	44.7	5.9
ARN	39.0	6.4	42.2	6.7	63.5	8.6	56.9	8.6	65.7	8.8
BOX	104.3	17.2	104.2	16.6	146.1	19.9	140.1	21.2	144.2	19.2
POX	73.4	12.1	75.6	12.1	61.0	8.3	69.1	10.5	61.4	8.2
SOX	157.6	26.0	157.9	25.2	167.9	22.8	147.7	22.4	169.2	22.5
ALH	9.4	1.5	11.0	1.8	15.3	2.1	10.4	1.6	14.7	2.0
AMH	10.0	1.7	10.3	1.7	12.7	1.7	12.9	1.9	13.1	1.7
ARH	8.7	1.4	10.0	1.6	13.2	1.8	12.3	1.9	12.7	1.7
PHO	1.7	0.3	1.8	0.3	0.8	0.1	1.6	0.2	0.5	0.1
Total	607.2		627.1		735.3		660.5		750.5	

* Average over the specified period.

ALC, aliphatic carbon; ARC, aromatic carbon; AMN, amino nitrogen; ARN, aromatic ring nitrogen; BOX, base carbonyl oxygen; POX, phosphate oxygen; SOX, sugar oxygen; ALH, aliphatic hydrogen; AMH, amino hydrogen; ARH, aromatic hydrogen; PHO, phosphate.

of the different atom types of the unstacked conformation has been analyzed during the periods of the MD simulation where the most extreme values of the accessible surface area occurred. The average accessible surface area was 660.5 Å² between 380 ps and 480 ps and 750.5 Å² from 960 ps to 1060 ps. We observed changes of about 2–3% for the aliphatic (ALC) and aromatic carbons (ARC) and for the base carbonyl (BOX) and phosphate oxygens (POX) by comparing these periods (Table 2). The major differences of the accessible surface area between the stacked and the unstacked conformation were the larger relative exposure of the aliphatic carbons (ALC), the sugar (SOX) and the phosphate oxygens (POX) for the stacked conformation. The contributions of the accessible surface area from the amino, the aromatic, and the aliphatic hydrogens were about 1–2% for both the stacked and the unstacked conformation.

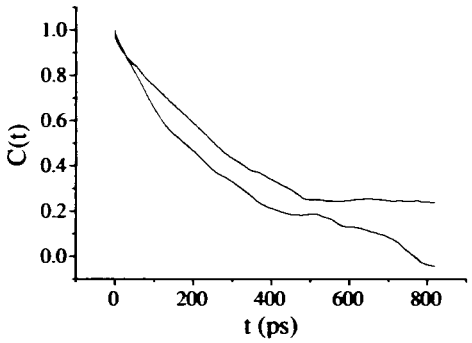

FIGURE 6 The correlation function of the vector between two atoms of the uridine moiety the O3′ atom and the C4′ atom (*top curve*) and of the vector between the N1 atom and the N9 atom of the guanine base (*bottom curve*) in the unstacked conformation.

Reorientation correlation functions

From the MD simulations the reorientational correlation functions have been calculated using Eq. 4 for different vectors to examine the mobility of both the bases and the sugar moieties of the dinucleoside monophosphate GpU. From the correlation function of a vector between two atoms in the guanine base, the N1 atom and the N9 atom, rotational correlation times of 107 ps for the stacked conformation (Fig. 5) and of 272 ps for the unstacked form (Fig. 6) have been determined.

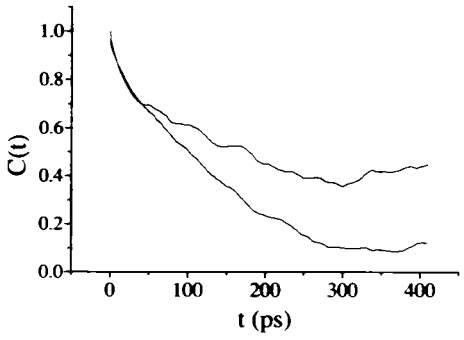

FIGURE 5 The correlation function of the vector between the N1 atom and the N9 atom of the guanine base (*top curve*) and of the vector between the O3′ atom and the C4′ atom of the uridine moiety (*bottom curve*) in the stacked conformation.

The mobility of the sugar moieties have been examined by placing a vector between the O3′ and the C4′ atom to cover possible conformational changes. The correlation time of rotation for the sugar moiety of the Urd base was 151 ps for the stacked conformation (Fig. 5) and 264 ps for the unstacked (Fig. 6).

The calculated correlation function was sensitive to how the vector was placed in the molecule and that made the estimated correlation time of rotational diffusion uncertain. The correlation time for the C2-C8 vector of the Gua base has been calculated to show the variety of these values (Table 3). These effects are depending on the incomplete sampling of the correlation functions especially for the unstacked conformation.

TABLE 3 Correlation times (ps) of rotational diffusion

	Stacked conformation	Extended conformation	Exp. GpU	
			G	U
Vector				
N1(Gua)-N9(Gua)	107	272		
C2(Gua)-C8(Gua)	123	198		
O3'(Urd)-C4'(Urd)	151	264		
Fluorescence			140*	
NMR			120‡	95‡
NMR			116§	92§
Hydrodynamic model				
(r_G)	52	61–168		
Intramolecular distance	134	169¶ 120‖		

* For 2-amino-purine uracil, from R. Rigler and T. Kulinski

‡ From Chachaty et al. (1977).

§ For 5'-GMP and 5'-UMP, from Chachaty et al. (1976).

¶ Around the short semiaxis *b*.

‖ Around the long semiaxis *a*.

Spin-lattice relaxation studies (Chachaty et al., 1976) have shown that the correlation times of purine and pyrimidine 5'-nucleotides varies from 91 to 120 ps. From the NMR study of GpU (Chachaty et al., 1977) rotational correlation times for Gp of 120 ps and for pU of 95 ps were obtained. The observed correlation times of UpG were shorter than for GpU, 90 ps for Up and 92 ps for pG. The rotational correlation time of the dinucleoside monophosphate 2-amino purine uracil, which has been studied using fluorescence spectroscopy measurements (R. Rigler and T. Kulinski, personal communication), was 140 ps. The correlation times calculated from the MD simulation of the stacked conformation using different vectors are in the same range as the experimental data, but the correlation times of the unstacked conformation are all longer.

The hydrodynamic model has been used to calculate rotational properties of molecules (Cantor and Schimmel, 1980). If we approximated the Stokes effective radius with the average radius of gyration, which was 4.02 Å, we got a correlation time of rotational diffusion of 52 ps. This value is too small due to that the radius of gyration is shorter than the Stokes effective radius, but if we instead used half the longest intramolecular distance 5.50 Å the correlation time was 134 ps. The correlation time from the hydrodynamic model derived from half the longest intramolecular distance of the stacked spherical conformation was in agreement with experimental data (Table 3). The unstacked conformation was assumed to have the shape of a prolate ellipsoid with two semiaxes, *a* and *b*. If these semiaxes were approximated with the longest intramolecular distances, the length *a* and the diameter *b* would be 8.16 Å and 4.18 Å, respectively. Using these data and Eqs. 5–7 we calculated the correlation times for rotation about the *a* and the *b* semiaxes to be 120 ps and 169 ps. It is clear that the estimations using the hydrodynamic model with these molecular dimensions give too low values for the rotational correlation times compared to the MD simulation.

Stacking

To investigate the stacking ability of the dinucleoside monophosphate GpU we calculated the distance between the N1 atom of the uracil base and the N9 atom of the guanine base. The stacked conformation was very well preserved through the whole MD simulation of 1.0 ns (Fig. 7 *a*), where the average of the N1-N9 distance over the last 400 ps was 4.39 Å with a RMS fluctuation of 0.34 Å. No water molecules were ever observed between the bases of the stacked conformation. From the 200 ps MD simulation of the deoxy form of GpU we observed that the conformation was remained stacked all the time.

The MD simulation of the unstacked starting conformation instead showed large fluctuations of the N1-N9 distance (Fig. 7 *b*). In this case the distance between the bases was around 9.3 Å the first 200 ps and thereafter the dinucleoside monophosphate transformed nearly into a stacked conformation after another 80 ps. This conformation did not stack quite as well as the stacked conformation, instead the N1-N9 distance was 1.7 Å larger. This more stacked conformation was kept until 580 ps and then an unfolding process back to an unstacked conformation started. At around 950 ps the distance between the bases was even longer than at the start of the MD simulation. Between 1080 ps and 1290 ps another conformational change appeared and thereafter nearly the same distance between the bases was reached as was used at the start of the MD simulation. During this very long 2.0-ns MD simulation the unstacked conformation adopted a lot of very different conformations. The distribution of the distance between the N1 atom of the uracil base and the N9 atom of

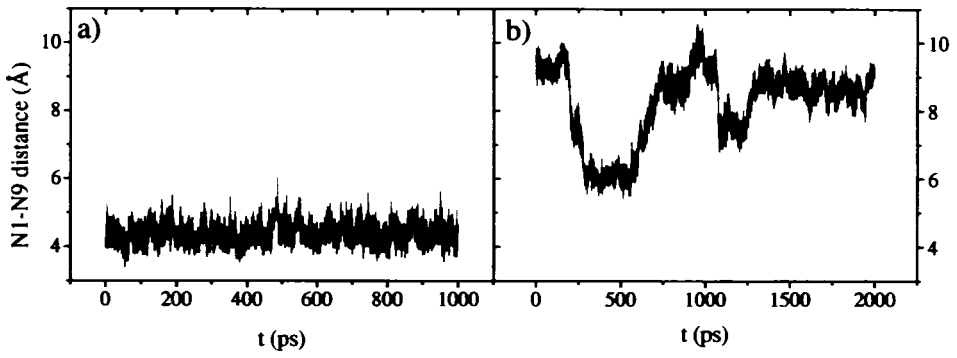

FIGURE 7 The time evolution of the distance between the N1 atom of uracil base and the N9 atom of guanine base for the stacked (*a*) and the unstacked (*b*) conformation.

the guanine base from the MD simulations of the stacked and the unstacked conformation showed two large peaks and two smaller (Fig. 8) at 4.4 Å, 6.1 Å, 7.5 Å, and 8.8 Å.

One model, which has been used to study the stacking-unstacking equilibrium of dinucleoside monophosphates is the two-state model (Davis and Tinoco, 1968), in which there are only two conformations, either the stacked or the unstacked conformation. At low temperatures the stacked conformation is favored, but at increasing temperature the equilibrium is shifted toward the unstacked conformation. The two conformations, either the ordered stacked conformation or the disordered unstacked conformation, are proposed to exist in equilibrium with each other, *Stacked* ↔ *Unstacked*, with some equilibrium constant $K(T)$ depending on the temperature (Bloomfield et al., 1974):

$$K(T) = \frac{\text{Fraction stacked}}{\text{Fraction unstacked}} = \frac{\phi(T) - \phi_u}{\phi_s - \phi(T)} \quad (8)$$

where $\phi(T)$ represents some measured property of the molecule at temperature T, for example the rotation of a molecule, ϕ_s and ϕ_u are the properties of the completely stacked and unstacked conformations, both at temperature T. Once the equilibrium constant is known the thermodynamic parameters for the transition from stacked to unstacked can be calculated using:

$$-RT \ln K = \Delta H - T\Delta S \quad (9)$$

where R is the gas constant, ΔH is the change of the enthalpy, and ΔS is the change of the entropy. Experimentally it may be difficult to obtain the properties ϕ_s and ϕ_u. The validity of the two-state model has been discussed (Davis and Tinoco, 1968; Bloomfield et al., 1974) and has also been shown to be satisfied only under certain conditions (Reich and Tinoco, 1980). The two-state model has been used for calculating thermodynamic parameters of the stacking-unstacking process of GpU (Davis and Tinoco, 1968; Guschlbauer et al., 1972; Guschlbauer, 1976), but the absence of detailed knowledge of the structure of the GpU makes the thermodynamic data based on the two-state model doubtful. The equilibrium constants of GpU from melting curves are between 0.26 and 0.37 (Guschlbauer et al., 1972) and about 0.31 from ORD experiment (Davis and Tinoco, 1968). Using this model for the calculation of the equilibrium constant from the correlation times derived from two vectors of the guanine base, the N1-N9 vector and the C2-C8 vector, and using the fluorescence experimental data as $\phi(T)$ (Table 3) gave equilibrium constants of 4.0 and 3.4, corresponding to 75–80% fraction stacked conformers which should be compared to 25–35% obtained from the CD and ORD equilibrium constants. Since the fluorescence anisotropy measurement is sensitive to the overall shape of the molecule, rather than to electronic interactions, these results indicate that there are compact, but not necessarily stacked conformations, that are populated a significant amount of time. Such conformations, as seen in the unstacked simulation during the period when the bases were close but not parallel (Figs. 7 *b* and 9 *d*), would give short rotational diffusion times, and still not contribute to the stacked conformations seen with the other techniques.

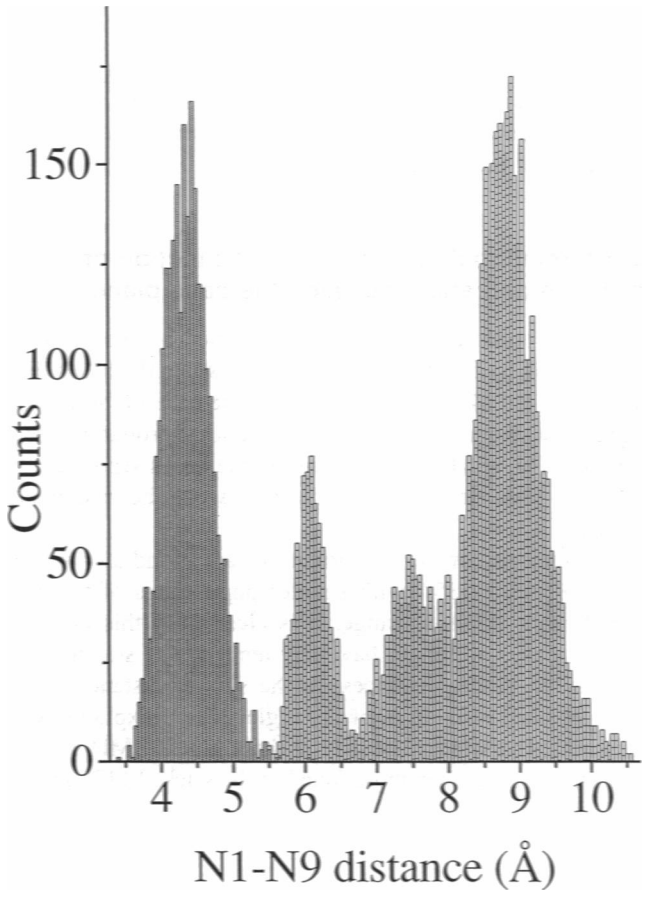

FIGURE 8 The distribution of the N1–N9 distance from the MD simulation for the stacked (*gray*) and the unstacked (*lined bars*) conformation.

Dipole moment

The total dipole moment at time t was calculated according to

$$M(t) = \sum_{i=1}^{n} q_i r_i(t) \quad (10)$$

where q_i is the charge of the atom i, n is the number of atoms and r_i is the distance from the center of mass to atom i. The total dipole moment of a single nucleotide base is much smaller than for a stacked dinucleoside monophosphate: 7.5 D for the guanine base and 4.6 D for the uracil base (Saenger, 1988) compared to the average total dipole moment of 21.6 D during the last 400 ps for the stacked conformation (Fig. 9 *a*), which also involves the sugar moieties and the phosphate. The RMS fluctuation was 1.6 D over the last 400 ps.

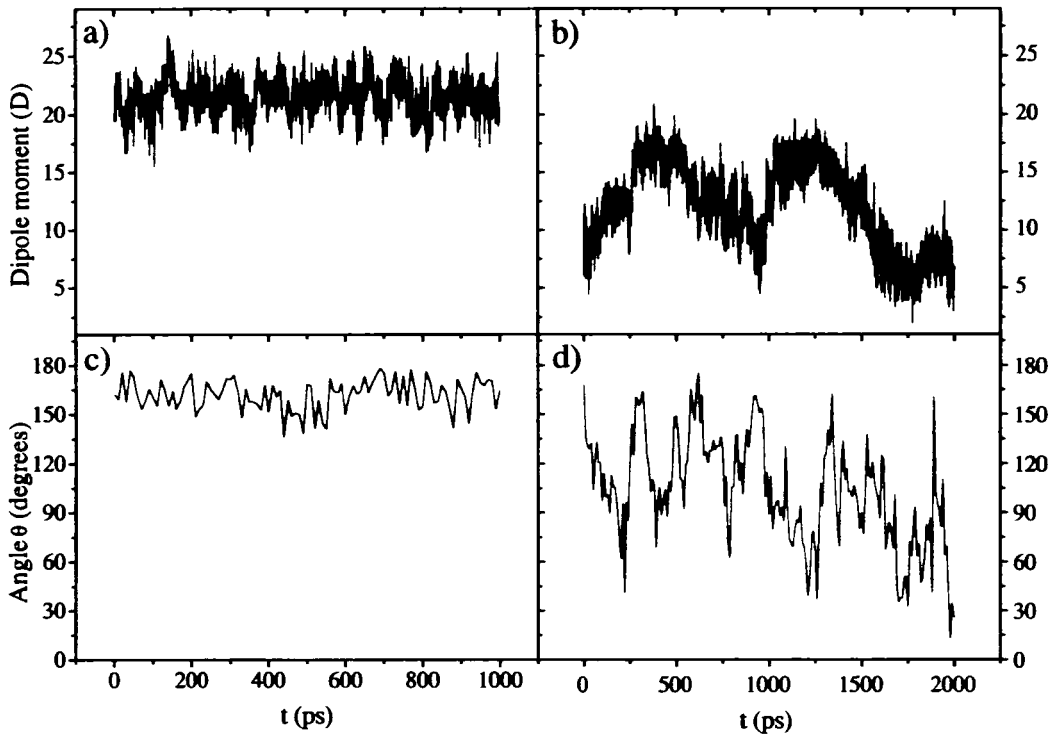

FIGURE 9 The total dipole moment in Debye (D) of the dinucleoside monophosphate GpU as a function of time for the stacked (*c*) and the unstacked (*d*) conformation and the angle θ between the normal vectors of the guanine base and of the uracil base vs. time for the stacked (*a*) and the unstacked (*b*) conformation.

On the other hand, the total dipole moment of the unstacked conformation, plotted in Fig. 9 *b*, fluctuated between 20.9 D and 2.0 D. The total dipole moment increased during the first 290 ps, but started to decrease from 520 ps until 950 ps. Thereafter the total dipole moment increased again to an average of 16.1 D (1100–1300 ps) and then followed a decreasing period, from 1300 ps to 1780 ps, to as low as 2.0 D due to the transition of the χ torsion angle of the guanosine moiety (Fig. 2 *d*). During the last 200 ps a small increase of the total dipole moment was observed depending on a transition of the χ torsion angle of the uridine moiety. The total dipole moment from the MD simulation of the unstacked conformation is smaller than for the MD simulation of the stacked conformation because of the charge symmetry of the unstacked conformation, giving a small dipole moment due to the fact that the positive and negative centers of the net charge are very close in space.

Angle between normal vectors of the bases

The orientation of the bases relative each other has been calculated using the angle θ between the normal vectors of the bases. The bases are exactly parallel when θ is 180°. In the stacked conformation there were no large fluctuations of the bases relative each other due to the very stable and stacked structure with the bases parallel throughout the MD simulation (Fig. 9 *c*), resulting in an average angle θ of 164.9° ± 8.9° during the last 400 ps. The angle θ of the MD simulation of the unstacked conformation (Fig. 9 *d*) showed major changes. We observed that during the stacking period from 280 ps to 580 ps, the bases were parallel (as in the stacked case) about 27% of the time. The major changes of the χ torsion angles could directly be seen from the time evolution of the angle θ.

Conformational distribution as a function of distance and angle between the base planes

The GpU conformations can be described by the distance (Figs. 7 and 8) and the angle (Fig. 9) between the bases. For the unstacked MD simulation, where the base mobility was significant, we have also analyzed the joint probability distribution $P(r, \theta)$ (Fig. 10) of finding the bases separated by a N1-N9 distance r and an angle θ between the base plane normals.

The majority of the conformations are found at r = 8–9 Å and θ = 75–135°, with smaller populations of the r = 6–8 Å, θ = 75–135° range. It is clear from this analysis that the bases no longer have any tendency of staying parallel at the longer distances. In the shorter distance range the bases are also often at an angle, which explains why the shortest distances obtained in the unstacked MD simulation are all longer than those found in the stacked MD simulation (Fig. 7).

Hydrogen bonds

The 2′-hydroxyl group of the ribose moiety plays an important role in the conformational stability of the oligo- and

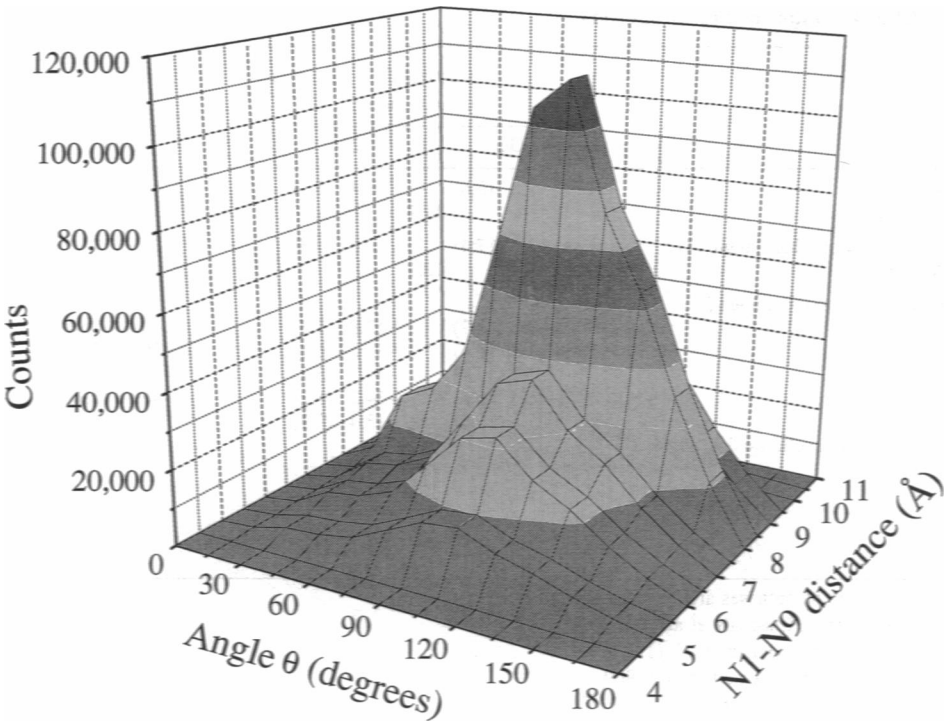

FIGURE 10 Conformational probability distribution as a function of the N1-N9 distance and the angle between the base plane normals for the unstacked MD simulation.

polynucleotides (Maurizot et al., 1969). This has been explained by the formation of a hydrogen bond between the 2′-OH group and the O4′ atom in the neighboring base (Saenger, 1988). The existence of this 2′-OH group explains the differences in conformational stability and physical properties of RNA and DNA (Bolton and Kearns, 1978). In the MD simulation of the stacked conformation we have seen that the hydrogen bond between the 2′-OH group of the Guo moiety and the O4′ atom of the Urd moiety is very important (Fig. 11).

A hydrogen bond with the H···X distance shorter than 1.95 Å is defined as strong and between 1.95 and 2.20 Å as weak. The O4′···O2′-H2′ hydrogen bond is strong 70.3% of the MD simulation and week 12.4%. Other hydrogen bonds have also been observed in the stacked conformation but only short times, for instance the O2···H2-N2 bonds, the O4′-(Urd)···H2-N2 bond, the O5′(Urd)···H2′-O2′(Guo) bond and the O6···H3-N3 bond. The O4′···O2′-H2′ hydrogen bond could of course not be observed in the deoxy form of the GpU, but still the stacked form was kept. In the MD

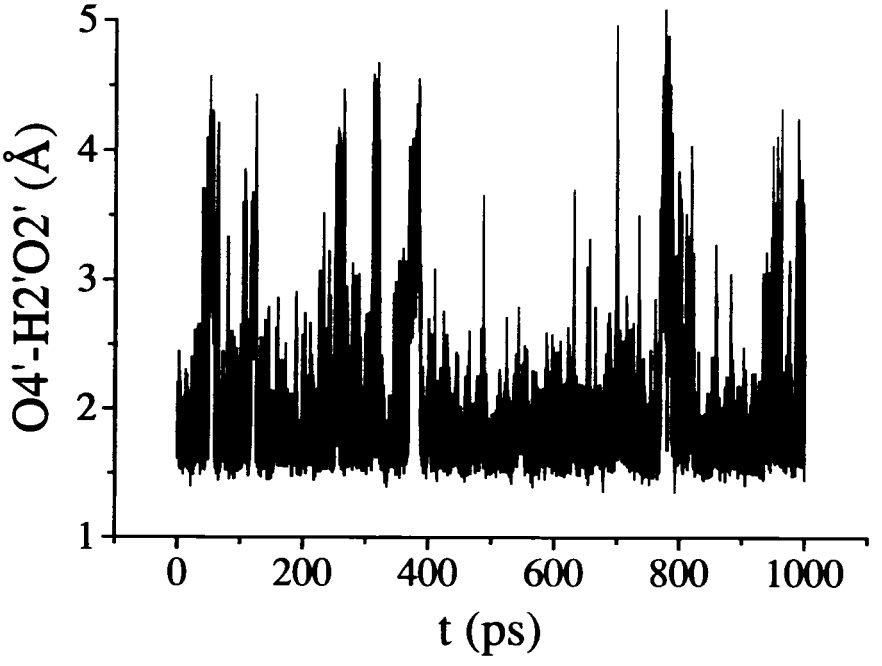

FIGURE 11 The time evolution of the O4′···H2′-O2′ hydrogen bond of the stacked conformation.

TABLE 4 Sugar pucker properties

	Stacked conformation		Extended conformation				
	Guo	Urd	Guo	Urd	Exp.		
υ_m (°)	41.8 (5.6)	40.4 (5.1)	46.7 (5.4)	39.7 (5.0)	38*		44‡
Average	41.1		43.2		38.8§		42.0¶
Pseudorotation phase angle (°)	2.6 (17.4)	0.6 (10.8)	29.9 (13.9)	2.6 (11.4)			
Average	12.1		16.2		4.5¶	10.5§	13.8
Endocyclic torsion angles (°)							
υ_0	−3.8 (12.7)	12.8 (7.3)	−9.0 (10.9)	11.3 (7.6)			
υ_1	−21.3 (10.5)	−33.2 (6.1)	−20.0 (9.7)	−31.9 (6.2)			
υ_2	36.3 (6.4)	39.7 (5.2)	39.2 (6.6)	38.9 (5.1)			
υ_3	−40.4 (6.8)	−34.2 (6.2)	−46.5 (6.1)	−34.5 (6.3)			
υ_4	27.8 (10.8)	13.4 (7.3)	35.0 (9.0)	14.3 (7.5)			
Average endocyclic torsion angles (°)							
υ_0	4.5		1.1		3.2		
υ_1	−27.3		−26.0		−25.6		
υ_2	38.0		39.0		36.9		
υ_3	−37.3		−40.5		−35.9		
υ_4	20.6		24.6		20.8		

Values in the parentheses are standard deviations.
* For Guo, from Chachaty et al. (1977).
‡ For Urd, from Chachaty et al. (1977).
§ For A-RNA, from Arnott et al. (1969).
¶ For A-RNA from Langridge et al. (1960).
For A-RNA, from Arnott et al. (1972).

simulation of the unstacked conformation weak hydrogen bonds, like the OP···H2′-O2′ bond, were observed during short periods. During the last part of the MD simulation weak hydrogen bonds, the OP···H2-N2 bond and the O5′(Urd)···H2-N2 bonds, were observed due to the transition of the χ torsion angle of the Guo moiety (Fig. 2 *d*). The GpU-water interactions will be analyzed elsewhere.

Sugar conformations

The endocyclic torsion angles have been defined as by Saenger (1988) and analyzed the last 400 ps. The average of each endocyclic torsion angle of the GpU (Table 4) in both the MD simulations is in good agreement with the data of the ribose ring of A-RNA (Arnott et al., 1972).

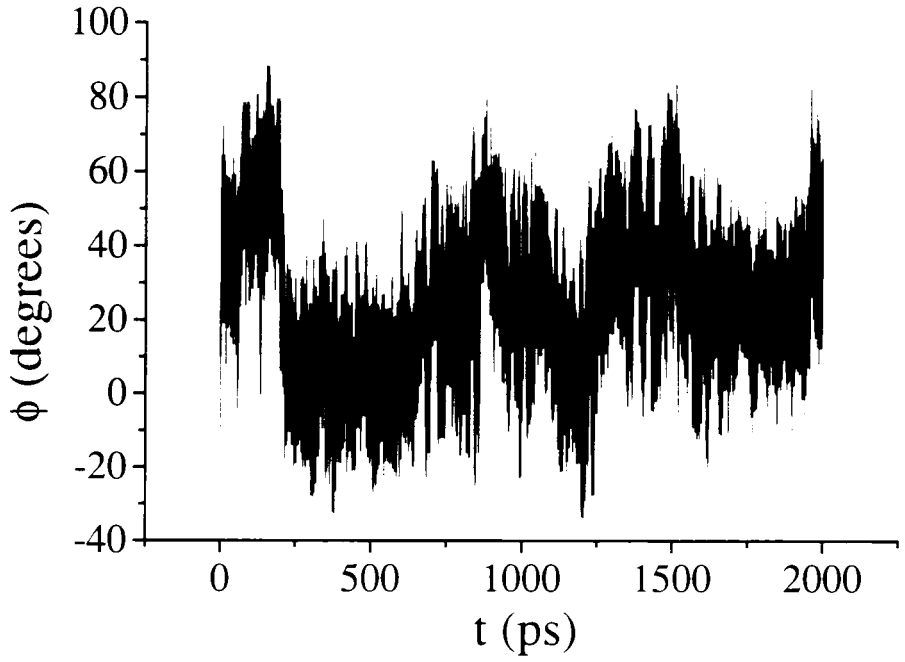

FIGURE 12 The time evolution of the pseudorotational phase angle ϕ for the guanosine moiety of the unstacked conformation.

Ribose puckering has been extensively examined using vacuo molecular dynamics simulations (Harvey and Prabhakaran, 1986), showing that different descriptions of the furanose ring conformation, based on the concept of pseudorotation, give very similar results. We follow Altona and Sundaralingam (1972) and describe the sugar conformation with two parameters, the phase angle of pseudorotation, ϕ, and the degree of pucker, υ_{max}:

$$\tan \phi = \frac{(\upsilon_1 + \upsilon_4) - (\upsilon_0 + \upsilon_3)}{2\upsilon_2(\sin 36° + \sin 72°)} \quad (11a)$$

$$\upsilon_{max} = \frac{\upsilon_2}{\cos \phi} \quad (11b)$$

where υ_i are the endocyclic torsion angles (Table 4).

The ribose ring of A-RNA is in the C3′-endo mode (Arnott et al., 1972), and in both the MD simulations the N form (−90° to 90°) of the phase angle of pseudorotation predominates, as is seen in Fig. 3, *a* and *b*. In the simulation of the stacked conformation the sugar puckering mode of the Urd moiety was all the time between the C2′-exo and the C3′-endo modes, with ϕ fluctuating around an average of 0.6°; the Guo moiety adopted the same modes as the Urd moiety, and also the C4′-exo mode, giving 17.4° RMS fluctuations of the ϕ angle of the Guo base, compared to 10.8° for the Urd base. The ribose ring of the Urd moiety in the MD simulation of the unstacked conformation fluctuated from the C2′-exo mode over the C4′-exo to a value between the C3′-endo and the C2′-exo modes. The Guo moiety also showed fluctuations between different modes, the C2′-exo, the C3′-endo, the C4′-exo and the O4′-endo modes (Fig. 12).

The Guo moiety fluctuated between the C3′-endo and the C4′-exo modes during the last 400 ps with an average of 29.9°. By NMR (Chachaty et al., 1977) it has been shown that in the Guo moiety the S form predominates and in the Urd moiety the N form predominates. The average of υ_{max} from the MD simulation of the stacked and the unstacked conformation showed values (Table 4) close to the proposed values for A-RNA (Arnott et al., 1969; Arnott et al., 1972; Langridge et al., 1960). The υ_{max} angle of the Guo moiety in both the MD simulations was too large compared with NMR data (Chachaty et al., 1977), whereas for the Urd moiety it was too small (Table 4).

CONCLUSIONS

We observed a wide range of different conformations from the two MD simulations, both stacked and unstacked, the conformational space of the MD simulation of the unstacked conformation was probably still not fully covered, even though it was extended to 2 ns. The softest internal degrees of freedom for GpU were the sugar pucker, the glycosidic torsions, and the backbone torsions α, β, ϵ, and ζ. The simulation starting from a stacked conformation remained stacked throughout, consistent with potential of mean force calculations (J. Norberg and L. Nilsson, manuscript in preparation) indicating a barrier of about 5 kcal/mol for the unstacking process. The dipole moment of the unstacked conformation was observed to be smaller than for the stacked form due to the charge symmetry. The O2′-H2′···O4′ hydrogen bond, which could be observed 82.7% of the MD simulation, may contribute to the stability of the stacked conformation, but could naturally not be observed in the MD simulation of the deoxy form of GpU, which nevertheless also stayed stacked. Rotational diffusion correlation times for GpU were calculated and found to be similar to experimental values, especially for the stacked conformation, and by combining them with time resolved fluorescence data a stacking equilibrium constant around 3–4 was obtained .

We thank Dr. W. Guschlbauer for discussion of earlier work on the dinucleotide GpU and Dr. T. Kulinski and Prof. R. Rigler for experimental results. This work was supported by the Swedish Natural Science Research Council and the Magnus Bergvall Foundation.

REFERENCES

Alden, C. J., and S.-H. Kim. 1979. Solvent-accessible surfaces of nucleic acids. *J. Mol. Biol.* 132:411–434.

Altona, C., and M. Sundaralingam. 1972. Conformational analysis of the sugar ring in nucleosides and nucleotides. A new description using the concept of pseudorotation. *J. Am. Chem. Soc.* 94:8205–8212.

Arnott, S., S. D. Dover, and A. J. Wonacott. 1969. Least-squares refinement of the crystal and molecular structures of DNA and RNA from x-ray data and standard bond lengths and angles. *Acta Crystallogr. Sect. B.* 25: 2192–2206.

Arnott, S., D. W. L. Hukins, and S. D. Dover. 1972. Optimised parameters for RNA double-helices. *Biochem. Biophys. Res. Commun.* 48: 1392–1399.

Arnott, S., P. J. C. Smith, and R. Chandrasekaran. 1976. Atomic coordinates and molecular conformations for DNA-DNA, RNA-RNA, and DNA-RNA helices. *In* CRC Handbook of Biochemistry and Molecular Biology: Nucleic Acids, 3rd ed., Vol. 2, G. D. Fasman, editor. CRC Press, Cleveland, OH. 411–422.

Bloomfield, V. A., D. Crothers, and I. Tinoco Jr. 1974. Physical Chemistry of Nucleic Acids. Harper and Row, New York.

Bolton, P. H., and D. R. Kearns. 1978. Hydrogen bonding of the 2′OH in RNA. *Biochim. Biophys. Acta.* 517:329–337.

Brooks, B. R., R. E. Bruccoleri, B. D. Olafson, D. J. States, S. Swaminathan, and M. Karplus. 1983. CHARMM: a program for macromolecular energy, minimization, and dynamics calculations. *J. Comp. Chem.* 4: 187–217.

Brooks III, C. L., M. Karplus, and B. M. Pettitt. 1988. Proteins: a Theoretical Perspective of Dynamics, Structure, and Thermodynamics. John Wiley & Sons, New York.

Cantor, R. C., and P. R. Schimmel. 1980. Biophysical Chemistry. W. H. Freeman, San Francisco.

Chachaty, C., T. Yokono, S. Tran-Dinh, and W. Guschlbauer. 1977. Oligonucleotide conformations. 5. NMR and relaxation studies on GpU and UpG at neutral pH. *Biophys. Chem.* 6:151–159.

Chachaty, C., T. Zemb, G. Langlet, S. Tran-Dinh, H. Buc, and M. Morange. 1976. A proton-relaxation-time study of the conformation of some purine and pyrimidine 5′-nucleotides in aqueous solution. *Eur. J. Biochem.* 62: 45–53.

Davis, R. C., and I. Tinoco Jr. 1968. Temperature-dependent properties of dinucleoside phosphates. *Biopolymers.* 6:223–242.

De Loof, H., L. Nilsson, and R. Rigler. 1992. Molecular dynamics simulation of galanin in aqueous and non-aqueous solution. *J. Am. Chem. Soc.* 114:4028–4035.

DiCapua, F. M., S. Swaminathan, and D. L. Beveridge. 1991. Theoretical evidence for water insertion in α-helix bending: molecular dynamics of Gly30 and Ala30 in vacuo and in solution. *J. Am. Chem. Soc.* 113: 6145–6155.

Guschlbauer, W. 1976. Nucleic Acid Structure. Springer-Verlag, New York.

Guschlbauer, W., I. Frič, and A. Holý. 1971. On the structure of guanyl 3'-5' uridine (GpU). *1st Eur. Biophys. Congr. (Symp. Y VI-A-5) Proc.* 1: 299–302.

Guschlbauer, W., I. Frič, and A. Holý. 1972. Oligonucleotide conformations. Optical studies on GpU analogues with modified-uridine residues. *Eur. J. Biochem.* 31:1–13.

Harvey, S. C., and M. Prabhakaran. 1986. Ribose puckering: structure, dynamics, energetics, and the pseudorotation cycle. *J. Am. Chem. Soc.* 108: 6128–6136.

Hu, Y., and G. R. Fleming. 1991. Molecular dynamics study of rotational reorientation of tryptophan and several indoles in water. *J. Chem. Phys.* 94:3857–3866.

Hunter, C. A. 1993. Sequence-dependent DNA structure. The role of base stacking interactions. *J. Mol. Biol.* 230:1025–1054.

Ichiye, T., and M. Karplus. 1983. Fluorescence depolarization of tryptophan residues in proteins: a molecular dynamics study. *Biochemistry.* 22: 2884–2893.

Jorgensen, W. L., J. Chandrasekhar, J. D. Madura, R. W. Impey, and M. L. Klein. 1983. Comparison of simple potential functions for simulating liquid water. *J. Chem. Phys.* 79:926–935.

Langlet, J., P. Claverie, F. Caron, and J. C. Boeuve. 1981. Interactions between nucleic acid bases in hydrogen bonded and stacked configurations: the role of the molecular charge distribution. *Int. J. Quant. Chem.* 19:299–338.

Langridge, R., D. A. Marvin, W. E. Seeds, H. R. Wilson, C. W. Hooper, M. H. F. Wilkins, and L. D. Hamilton. 1960. The molecular configuration of deoxyribonucleic acid. II. Molecular models and their Fourier transforms. *J. Mol. Biol.* 2:38–64.

Lee, B., and F. M. Richards. 1971. The interpretation of protein structures: estimation of static accessibility. *J. Mol. Biol.* 55:379–400.

Levitt, M. 1983. Computer simulation of DNA double-helix dynamics. *Cold Spring Harbor Symp. Quant. Biol.* 47:251–275.

Lysov, Y. P., V. B. Zhurkin, L. Yu. Tychinskaya, and V. L. Florent'ev. 1979. Eight types of stacking interactions in dinucleotides. Conformational analyses of ApA, ApC, CpA, CpC, AND GpG. *Mol. Biol. (Mosk.).* 13: 1161–1188.

Marshall, A. G. 1978. Biophysical Chemistry Principles, Techniques, and Applications. John Wiley and Sons, New York.

Maurizot, J. C., J. Brahms, and F. Eckstein. 1969. Forces involved in the conformational stability of nucleic acids. *Nature.* 222:559–561.

McCammon, J. A., and S. C. Harvey. 1987. Dynamics of Proteins and Nucleic Acids. Cambridge University Press, Cambridge.

Neumann, J.-M., W. Guschlbauer, and S. Tran-Dinh. 1979. Conformation and flexibility of GpC and CpG in neutral aqueous solution using ^{1}H nuclear-magnetic-resonance and spin-lattice-relaxation time measurements. *Eur. J. Biochem.* 100:141–148.

Nilsson, L., and M. Karplus. 1986. Empirical energy functions for energy minimization and dynamics of nucleic acids. *J. Comp. Chem.* 7:591–616.

Poltev, V. I., L. A. Milova, B. S. Zhorov, and V. A. Govyrin. 1981. Simulation of conformational possibilities of DNA via calculation of nonbonded interactions of complementary dinucleoside phosphate complexes. *Biopolymers.* 20:1–15.

Prabhakaran, M., S. C. Harvey, B. Mao, and J. A. McCammon. 1983. Molecular dynamics of phenylalanine transfer RNA. *J. Biomol. Struct. Dyn.* 1:357–369.

Ravishanker, G., S. Swaminathan, D. L. Beveridge, R. Lavery, and H. Sklenar. 1989. Conformational and helicoidal analysis of 30 ps of molecular dynamics on the d(CGCGAATTCGCG) double helix: "curves," dials and windows. *J. Biomol. Struct. Dyn.* 6:669–699.

Reich, C., and I. Tinoco Jr. 1980. Fluorescence-detected circular dichroism of dinucleoside phosphates. A study of solution conformations and the two-states model. *Biopolymers.* 19:833–848.

Ryckaert, J.-P., G. Ciccotti, and H. J. C. Berendsen. 1977. Numerical integration of the Cartesian equations of motion of a system with constraints: molecular dynamics of n-alkanes. *J. Comp. Phys.* 23:327–341.

Saenger, W. 1988. Principles of Nucleic Acid Structure. Springer-Verlag, New York.

Seibel, G. L., U. C. Singh, and P. A. Kollman. 1986. A molecular dynamics simulation of double helical B-DNA including counterions and water. *Proc. Natl. Acad. Sci. USA.* 82:6537–6540.

Soman, K. V., A. Karimi, and D. A. Case. 1991. Unfolding of an α-helix in water. *Biopolymers.* 31:1351–1361.

Tidor, B., K. K. Irikura, B. R. Brooks, and M. Karplus. 1983. Dynamics of DNA oligomers. *J. Biomol. Struct. Dyn.* 1:231- 252.

Tobias, D. J., J. E. Mertz, and C. L. Brooks III. 1991. Nanosecond timescale folding dynamics of a pentapeptide in water. *Biochemistry.* 30:6054–6058.

Ts'o, P. O. P., N. S. Kondo, M. P. Schweizer, and D. P. Hollis. 1969. Studies of the conformation and interaction in dinucleoside mono- and diphosphates by proton magnetic resonance. *Biochemistry.* 8:997–1029.

Ts'o, P. O. P., I. S. Melvin, and A. C. Olson. 1963. Interaction and association of bases and nucleosides in aqueous solutions. *J. Am. Chem. Soc.* 85:1289–1296.

van Gunsteren, W. F., and H. J. C. Berendsen. 1977. Algorithms for macromolecular dynamics and constraint dynamics. *Mol. Phys.* 34: 1311–1327.

van Gunsteren, W. F., H. J. C. Berendsen, R. G. Geurtsen, and H. R. J. Zwinderman. 1986. A molecular dynamics computer simulation of an eight-base-pair DNA fragment in aqueous solution: comparison with experimental two-dimensional NMR data. *Ann. N.Y. Acad. Sci.* 482:287–303.

Verlet, L. 1967. Computer "experiments" on classical fluids. I. Thermodynamical properties of Lennard-Jones molecules. *Phys. Rev.* 159: 98–103.

Warshaw, M. M., and I. Tinoco Jr. 1966. Optical properties of sixteen dinucleoside phosphates. *J. Mol. Biol.* 20:29–38.

Yathindra, N., and M. Sundaralingam. 1973. Conformational studies on guanosine nucleotides and polynucleotides. The effect of the base on glycosyl and backbone conformations. *Biopolymers.* 12:2075–2082.